*High-mass X-ray Binaries: Illuminating the Passage from Massive Binaries to Merging Compact Objects*
*Proceedings IAU Symposium No. 346, 2019*
*L. M. Oskinova, E. Bozzo, T. Bulik & D. Gies, eds.*


doi:10.1017/S1743921319000024

# Modeling of hydrodynamic processes within high-mass X-ray binaries

**Petr Kurfürst**[1,2] **and Jiří Krtička**[1]

[1]Department of Theoretical Physics and Astrophysics, Masaryk University, Kotlářská 2, CZ-611 37 Brno, Czech Republic
emails: petrk@physics.muni.cz, krticka@physics.muni.cz

[2]Institute of Theoretical Physics, Charles University, V Holešovičkách 2, 180 00 Praha 8, Czech Republic
email: petrk@physics.muni.cz

**Abstract.** High-mass X-ray binaries belong to the brightest objects in the X-ray sky. They usually consist of a massive O or B star or a blue supergiant while the compact X-ray emitting component is a neutron star (NS) or a black hole. Intensive matter accretion onto the compact object can take place through different mechanisms: wind accretion, Roche-lobe overflow, or circumstellar disk. In our multi-dimensional models we perform numerical simulations of the accretion of matter onto a compact companion in case of Be/X-ray binaries. Using Bondi-Hoyle-Littleton approximation, we estimate the NS accretion rate. We determine the Be/X-ray binary disk hydrodynamic structure and compare its deviation from isolated Be stars' disk. From the rate and morphology of the accretion flow and the X-ray luminosity we improve the estimate of the disk mass-loss rate. We also study the behavior of a binary system undergoing a supernova explosion, assuming a blue supergiant progenitor with an aspherical circumstellar environment.

**Keywords.** massive stars, evolution, mass-loss, accretion, supernovae

## 1. Be/X-ray binaries

X-ray emission in Be/X-ray binaries comes from accretion of the material of the disk onto neutron star (NS) (Reig 2011). Its binary separation $D$ provides, due to the disk truncation, the determining constraint on the outer disk radius. We employ Bondi-Hoyle-Littleton (BHL) approximation (excluding the cases of very small disk scale-height $H$ very close to the Be star, where BHL approximation may be an excessive simplification (Okazaki & Negueruela 2001)) where the NS accretes within the radius

$$r_{\rm acc} = \frac{2GM_X}{v_{\rm rel}^2}, \tag{1.1}$$

where $M_X$ is the mass of the NS and $v_{\rm rel}$ is the relative velocity of NS and the disk. We distinguish two limiting cases for the disk-NS systems (Krtička *et al.* 2015):

- the NS is corotating with the disk material, $v_{\rm rel} = v_R$,
- the disk is truncated far from NS; in this case $v_{\rm rel}^2 \approx v_R^2 + v_\phi^2$.

Figure 1 shows the accretion radii of the two cases up to the distance $R = 10^4\,R_\star$. In systems with low orbital eccentricity we expect the disk truncation at the $3:1$ resonance radius (Okazaki & Negueruela 2001), that is, $R_{\rm trunc}/D \approx 0.48$. If $r_{\rm acc}$ exceeds the disk scale-height $H$, the NS accretes all the disk material and the X-ray luminosity is

$$L_X = \frac{GM_X\dot{M}}{R_X}, \tag{1.2}$$

where $\dot{M}$ is the accretion rate and $R_X$ is the NS radius (Krtička *et al.* 2015).

**Table 1.** Parameters of selected Be/X-ray binaries

| Binary | Sp. Type | $T_{\rm eff}$ [kK] | $R$ [$R_\odot$] | $D$ [$R_\odot$] | $L_X$ [W] |
|---|---|---|---|---|---|
| V831 Cas | B1V | 24 | 4.5 | 480 | $2 \times 10^{28}$ |
| IGR J16393-4643 | BV | 24 | 4.5 | 18.8 | $4 \times 10^{28}$ |
| V615 Cas | B0Ve | 26 | 4.9 | 43 | $5 \times 10^{28}$ |
| HD 259440 | B0Vpe | 30 | 5.8 | 510 | $1.2 \times 10^{26}$ |
| HD 215770 | O9.7IIIe | 28 | 12.8 | 260 | $6.5 \times 10^{29}$ |
| CPD-632495 | B2Ve | 34 | 7.0 | 177 | $3.5 \times 10^{27}$ |
| GRO J1008-57 | B0eV | 30 | 5.8 | 390 | $3 \times 10^{30}$ |

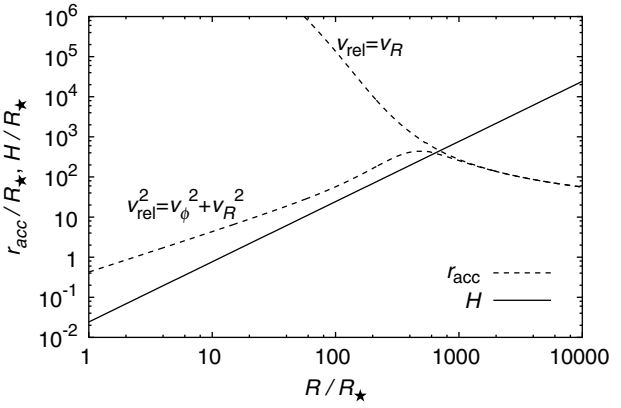


**Figure 1.** Comparison of $r_{\rm acc}$ and $H$ for a corotating NS ($v_{\rm rel} = v_R$) and for the case when the disk is truncated far from the NS, where $v_{\rm rel}^2 \approx v_R^2 + v_\phi^2$. Adapted from Krtička *et al.* (2015).

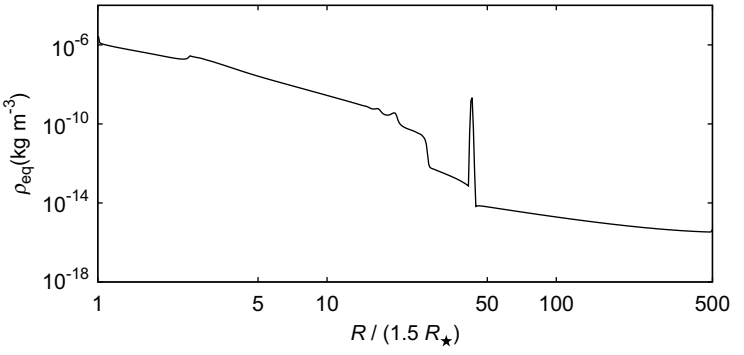


**Figure 2.** Disk midplane (equatorial plane) density profile $\rho_{\rm eq}$ in the direction of the corotating NS GROJ100857 (see Tab. 1), the parameters of the model are: $D \approx 67\, R_\star$, $T_{\rm eff} = 32\,000$ K, $L_X = 3 \times 10^{28}$ J s$^{-1}$, $r_{\rm acc}/H \propto 10^4$. The distance is scaled to the equatorial radius $R_{\rm eq}$ of a critically rotating star, $R_{\rm eq} = 1.5\, R_\star$.

We analyzed the sample of Be/X-ray binaries (see Tab. 1) for which $r_{\rm acc} > H$. With known X-ray luminosity we estimated from Eq. (1.2) $\dot{M} \sim 10^{-13}$ - $10^{-9}\, M_\odot\, {\rm yr}^{-1}$ (Krtička *et al.* 2015) for aligned systems. For the selected sample we calculated detailed self-consistent 2D numerical models of density and thermal structure of Be-stars' disk with included NS gravity and X-ray heating of the ambient disk gas, assuming vertical hydrostatic, thermal and radiative equilibrium (see examples for GRO J1008-57 in Figs. 2 and 3). Figure 2 shows that the disk density truncation in the disk - NS plane begins approximately at the expected resonance radius. We included the irradiative flux from the central star whose effects are calculated using method of short characteristics. We

https://doi.org/10.1017/S1743921319000024 Published online by Cambridge University Press

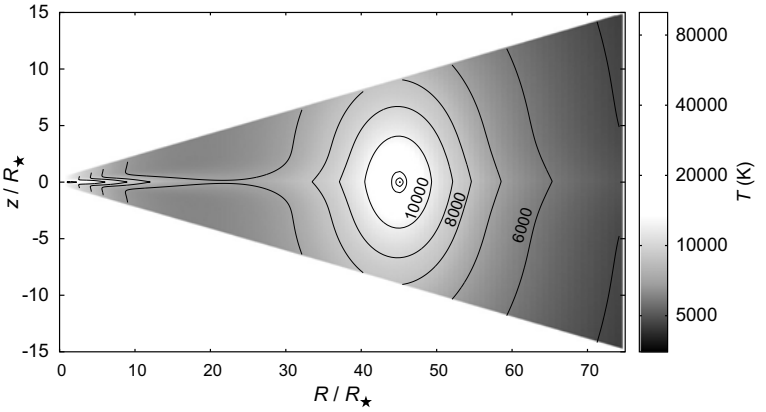


**Figure 3.** Thermal structure of the 2D model with the same parameters as in Fig. 2.

calculated the thermal and radiative flux near the disk midplane as a diffusion approximation. We used our own Eulerian hydrodynamic code and special cylindrical-conical coordinate system (Kurfürst *et al.* 2018).

## 2. Supernova explosion

We perform two separate models of interaction of an expanding supernova (SN) envelope with an asymmetric circumstellar medium (CSM) including a dense equatorial disk. We adopted the initial density and temperature profile of the progenitors from MESA model and SNEC code (Morozova *et al.* 2015). We assumed a spherically symmetric component of CSM (created, for example, by the stellar wind of the progenitor) with the initial density profile $\rho \propto r^{-2}$ while we input the disk component with a Gaussian vertical and radially decreasing density profile.

The upper panel of Fig. 4 shows the snapshot of the density structure in case of a blue supergiant (BSG) progenitor with parameters $M_\star = 40\,M_\odot$, $R_\star = 50\,R_\odot$, the explosion energy $E = 10^{44}$ J (where the total $\dot{M} = 10^{-1}\,M_\odot\,\mathrm{yr}^{-1}$), at time $t \approx 500$ hrs after the emergence of the shock. The velocities of the expansion front reach in this case values of approximately $2\,000\,\mathrm{km\,s^{-1}}$ in the polar direction $z$ and $1\,000\,\mathrm{km\,s^{-1}}$ in the equatorial direction $x$. The lower panel of Fig. 4 shows the snapshot of density structure in case of a BSG progenitor with parameters $M_\star = 40\,M_\odot$, $R_\star = 50\,R_\odot$, the explosion energy $E = 10^{44}$ J (where the total $\dot{M} = 10^{-2}\,M_\odot\,\mathrm{yr}^{-1}$), at time $t \approx 180$ hrs after the emergence of the shock. The velocities of the expansion front reach in this case values of approximately $4\,500\,\mathrm{km\,s^{-1}}$ in the polar direction $z$ and $1\,800\,\mathrm{km\,s^{-1}}$in the equatorial direction $x$. Due to interaction with asymmetric CSM the expanding SN envelopes are significantly aspherical toward large distances.

We investigate (see Fig. 5) the density and velocity profile in case of the interaction of the SN expanding envelope (of the BSG progenitor with the same parameters and the same CSM as in the lower panel of Fig. 4) with a binary companion with mass $M_\star = 8\,M_\odot$ (with uniform internal density for simplicity), with its own spherically symmetric CSM whose initial density profile is assumed as $\rho \propto r^{-2}$. The 1D snapshots show the values of density and expansion velocity at time $t \approx 50$ hrs after the emergence of the shock, when the shock front approximately reaches the distance of the companion, however, in later time the expansion velocity behind the companion increases up to the value of approximately $4\,500\,\mathrm{km\,s^{-1}}$, thus equating the shock front speed in the polar direction.

https://doi.org/10.1017/S1743921319000024 Published online by Cambridge University Press

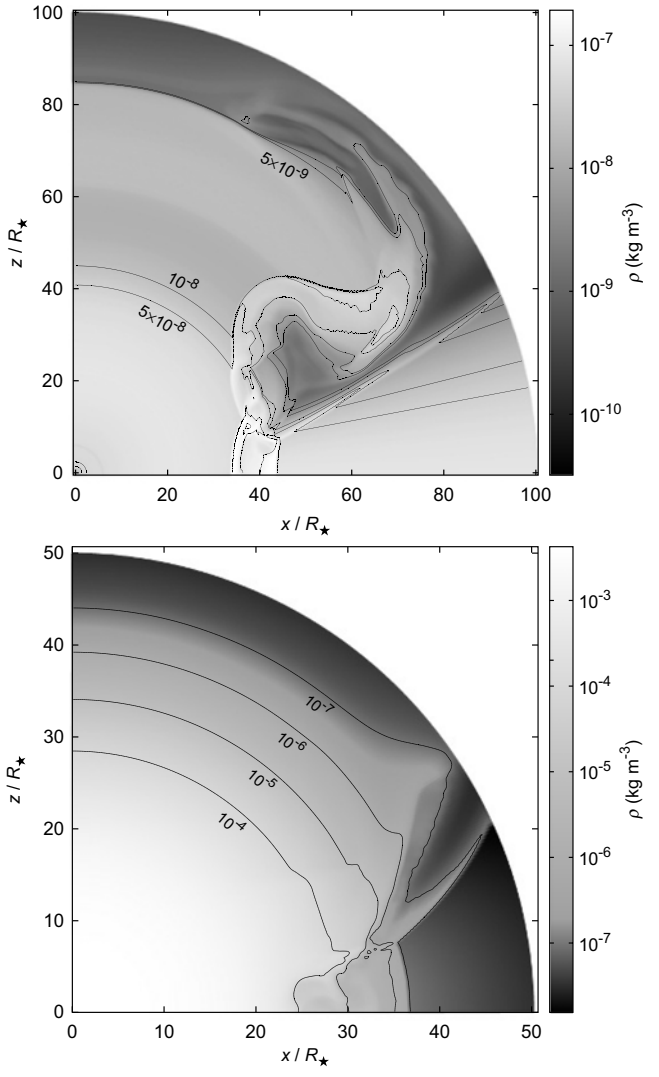


**Figure 4.** *Upper panel*: Density structure of the interaction of SN with asymmetric CSM that forms a dense equatorial disk (total $\dot{M} = 10^{-1}\, M_\odot\, \mathrm{yr}^{-1}$), at time $t \approx 500$ hrs after the emergence of the shock, the SN progenitor is a BSG star. *Lower panel*: Density structure of the BSG SN interaction with asymmetric CSM that forms a Keplerian equatorial disk (total $\dot{M} = 10^{-2}\, M_\odot\, \mathrm{yr}^{-1}$), at time $t \approx 180$ hrs after the emergence of the shock.

## 3. Conclusions

The corotating Be/X-ray binary models show that the inner disk structure is not affected significantly by presence of the NS companion and that the disk density truncation in the NS direction begins approximately at the 3:1 resonance radius (cf. Okazaki & Negueruela 2001). The disk is truncated relatively near the central star (inside the sonic point radius), therefore in case of a critically rotating star $\dot{M}$ should increase due to the angular momentum conservation. Future plans include calculations of models with eccentric and inclined (non-aligned) NS orbits and models where $r_{\mathrm{acc}} < H$.

The SN explosion models show the aspherical evolution of the density, velocity, and temperature of the ejecta that however in basic features confirm the analytic self-similarity relations developed, e.g., in Chevalier (1989). The dense equatorial disk and

https://doi.org/10.1017/S1743921319000024 Published online by Cambridge University Press

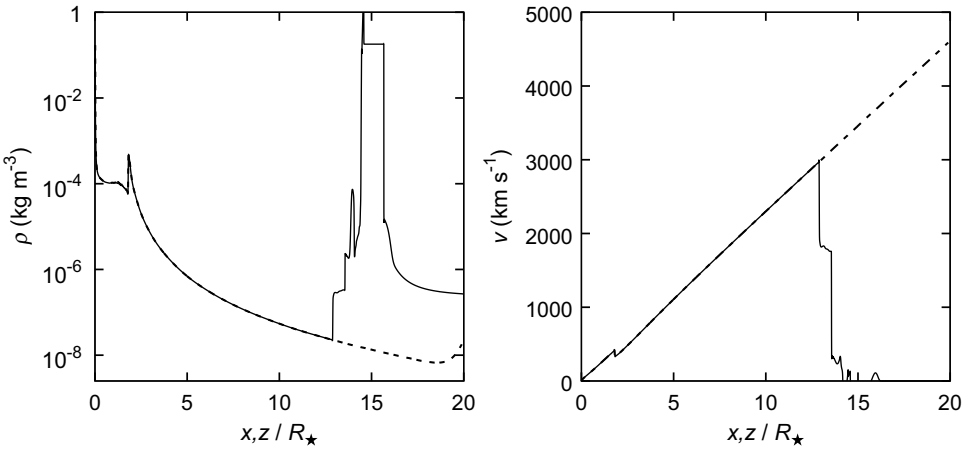


**Figure 5.** 1D slices of density (*left panel*) and velocity (*right panel*) in the plane of a companion star (*solid line*) and in the plane perpendicular to it (*dashed line*).

similarly the companion star may effectively block the SN expansion producing significantly over-dense and over-heated regions with developing Kelvin-Helmholtz and Rayleigh-Taylor instabilities.

## Acknowledgement

The access to computing facilities owned by the National Grid Infrastructure MetaCentrum, provided under 'Projects of Large Infrastructure for Research, Development, and Innovations' (LM2010005) is appreciated. This work was supported by grant GAČR 18-05665S.

## References

Chevalier, R. A. 1989, *ApJ*, 258, 790C
Krtička, J., Kurfürst, P., & Krtičková, I. 2015, *A&A*, 573, 20K
Kurfürst, P., Feldmeier, A., & Krtička, J. 2014, *A&A*, 569, 23K
Kurfürst, P., Feldmeier, A. & Krtička, J. 2018, *A&A*, 613, A75
Lee, U., Osaki, Y., & Saio, H. 1991, *MNRAS*, 250, 432L
Morozova, V., Piro, A. L., & Renzo, M. 2015, *ApJ*, 814, 63
Okazaki, A. T., & Negueruela, I. 2001, *A&A*, 377, 161
Reig, P. 2011, *Ap&SS*, 332, 1R
Rivinius, T., Carciofi, A. C., & Martayan, C. 2013, *A&ARv*, 21, 69R

https://doi.org/10.1017/S1743921319000024 Published online by Cambridge University Press